Am. J. Hum. Genet. 63:506–516, 1998

Assignment of the Disease Locus for Lethal Congenital Contracture Syndrome to a Restricted Region of Chromosome 9q34, by Genome Scan Using Five Affected Individuals

Päivi Mäkelä-Bengs,[1] Niklas Järvinen,[2] Katri Vuopala,[3,5] Anu Suomalainen,[1] Jaakko Ignatius,[4] Mari Sipilä,[1] Riitta Herva,[5] Aarno Palotie,[2] and Leena Peltonen[1]

[1]Department of Human Molecular Genetics, National Public Health Institute, and Department of Medical Genetics, University of Helsinki; [2]Department of Clinical Chemistry, University of Helsinki, Helsinki; [3]Department of Pathology, Lapland Central Hospital, Rovaniemi, Finland; [4]Department of Clinical Neurophysiology, Jorvi Hospital, Espoo, Finland; and [5]Department of Pathology, University of Oulu, Oulu, Finland

Summary

Lethal congenital contracture syndrome (LCCS) is an autosomal recessive disease leading to death before the 32d gestational week. It is characterized by the fetal akinesia phenotype, with highly focused degeneration of motoneurons in the spinal cord as the main neuropathological finding. We report here the assignment of the LCCS locus to a defined region of chromosome 9q34, between markers D9S1825 and D9S1830. The initial genome scan was performed with the DNA samples of only five affected individuals from two unrelated LCCS families. The conventional linkage analysis performed with 20 affected individuals and their families was focused on those chromosomal regions in which the affected siblings were identical by descent in the initial scan. One core haplotype of 3 cM was observed in LCCS alleles, supporting the assumption of one major mutation underlying LCCS, and linkage disequilibrium analysis restricted the critical chromosomal region to <100 kb in the vicinity of marker D9S61. Two genes, NGAL (neutrophil gelatinase–associated lipocalin and NOTCH 1, were excluded as causative genes for LCCS

Introduction

Lethal congenital contracture syndrome (LCCS) is an autosomal recessive syndrome (MIM 253310) (Herva et al. 1985) leading to prenatal death of the affected fetus before the 32d week of gestation. The LCCS fetuses present with a typical fetal akinesia phenotype with multiple contractures of joints. The degeneration of descending tracts and anterior-horn motoneurons of the spinal cord is the main histopathological finding (Herva et al. 1988; Vuopala and Herva 1994). The etiology and pathological mechanism of LCCS are still unknown.

To date, a total of 43 LCCS cases have been reported, all from Finland. The disease-gene frequency is ~.0089 in Finland but is higher, ~.016, in the northeastern part of Finland, showing enrichment of the disease in the genetically isolated subpopulation of the later-settled area of this country (Vuopala and Herva 1994). In such a setting the disease can be assumed to be caused by a single major mutation, and linkage disequilibrium should be detectable by use of markers flanking the disease locus (Hästbacka et al. 1992). Consequently, the search for a shared chromosomal segment is the method of choice in the search for the disease locus, necessitating initial genotyping of only a small number of affected individuals (Houwen et al. 1994; Nikali et al. 1995).

Here we report the assignment of the LCCS locus by means of a genomewide scan based on the initial genotyping of five affected individuals from two families. Further linkage analyses in the complete study material of 10 families revealed evidence for linkage on 9q33-34. Two genes—NOTCH1 (Larsson et al. 1994) and NGAL (Chan et al. 1994)—that previously had been assigned to this chromosomal region were excluded as causative genes.

Subjects and Methods

Subjects

The 10 LCCS pedigrees used in this study are shown in figure 1. The mean gestational age of the fetuses was 27 wk. Growth retardation occurred during the second half of the gestation period, and the hydrops observed in early pregnancy disappeared during development. The typical LCCS phenotype included low-set and posteri-

Received February 27, 1998; accepted for publication June 12, 1998; electronically published July 17, 1998.

Address for correspondence and reprints: Dr. Leena Peltonen, Department of Human Molecular Genetics, National Public Health Institute, Mannerheimintie 166, FIN-00300 Helsinki, Finland. E-mail: leena.peltonen@ktl.fi

0002-9297/98/6302-0026$02.00

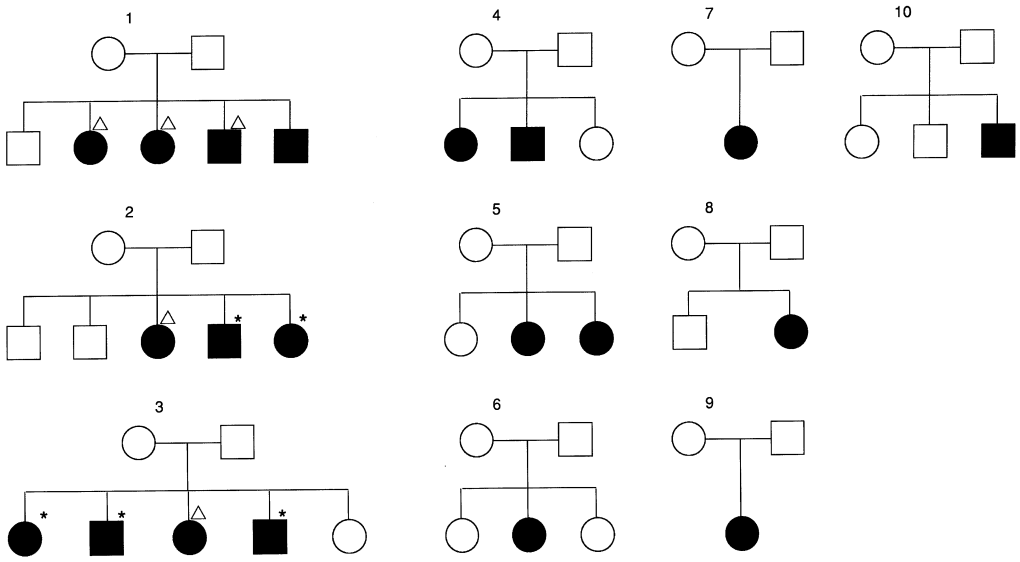

Figure 1 LCCS pedigrees. Blackened symbols denote affected individuals; asterisks denote affected individuals whose DNA samples were analyzed in the initial genome scan, and triangles denote individuals whose DNA was isolated from paraffin-embedded samples. DNA samples of all the family members from these 10 families were used for genotyping and in linkage analyses.

orly angulated ears, pterygia at the elbows, hypoplastic jaw, and sticklike extremities with multiple joint contractures. The autopsy showed pulmonary hypoplasia , skeletal muscle atrophy, and a marked reduction of motor neurons in the ventral part of the spinal cord. The rest of the CNS was intact. The spinal cord from at least one affected sibling in each family was available for neuropathological examination (Vuopala and Herva 1994; Vuopala et al. 1994). All samples were collected in accordance with the Helsinki Declaration.

DNA-Marker Analysis

Total DNA was extracted from the leukocytes of peripheral blood samples from the parents and their healthy offspring and from tissue samples or cultured cells of the LCCS fetuses, in accordance with standard procedures. Samples were available from 13 LCCS fetuses: fibroblasts from 7, liver tissue from 1, and placental tissue from 5. The paraffin-embedded tissue samples were available from seven affected fetuses. The age of the available paraffin-embedded tissues was 7–12 years. All the paraffin-embedded tissues were stored at room temperature. DNA extraction from paraffin-embedded tissues from four patients was kindly performed by Dr. K. Zerres. The other three samples were deparaffinized, and the DNA was released from cells by the rapid-lysis method (Isola et al. 1994). These samples increased significantly the informativeness of our family material.

The genomewide scan for linkage was performed by use of polymorphic tetra-, tri-, or dinucleotide DNA markers selected from either the Généthon primers collection or the Cooperative Human linkage Center (CHLC) (Sheffield et al. 1995). The primers for the CHLC markers either were purchased from the Nordic Human Genome Initiative or were synthesized in our laboratory by means of a 394 DNA/RNA Synthesizer (Applied Biosystem). The polymorphic dinucleotide repeats were amplified by PCR, and the products were separated either by PAGE, as described elsewhere (Vuopala et al. 1995), or on an automated laser-fluorescence DNA sequencer (ALF; Pharmacia); and the tetra- and trinucleotide markers were fluorescence 5′ end–labeled (with either FITC or cyp5), and the amplified PCR products were separated on an automated laser-fluorescence DNA sequencer (ALF; Pharmacia).

Linkage Analysis

To confirm that our study material was sufficient to provide conclusive evidence for linkage, the MSIM option of the SLINK computer program of the LINKAGE package was used (Ott 1989; Weeks et al. 1990). The parameters applied in linkage analyses were an autosomal recessive trait with .0089 gene frequency and, because of the lethality of the disease, complete penetrance. Five hundred replicates of the studied pedigrees revealed an average expected LOD score of 4.3, with an SD of 1.3 and a maximum LOD score of 6.5. Two-point

linkage analyses were performed by means of the MLINK option of the LINKAGE package, and multipoint analyses were performed by means of the LINKMAP option, version FASTLINK 2.2 (Lathrop and Lalouel 1984; Lathrop et al. 1984, 1986). The order and distances between the analyzed markers were based on either published marker maps (the Genetic Location Database; Généthon) or FISH analysis of metaphase chromosomes. The HOMOG program was used to test for locus heterogeneity (Ott 1986).

Linkage-Disequilibrium Analyses

The tests for allelic association were performed by means of the TDT LIKE and HRRLAMB programs (Nikali et al. 1995; Terwilliger 1995). The haplotype relative rate (HRR) analysis takes into account also the allele information from homozygous parents, which is excluded in the transmission/disequilibrium test (TDT) analysis. P_{excess} is calculated by means of the formula $P_{\text{excess}} = (P_{\text{affected}} - P_{\text{normal}})/(1 - P_{\text{normal}})$, in which P_{affected} is the allele frequency, among the disease chromosomes, of a marker locus descending from the ancestral haplotype and P_{normal} is the frequency of the same allele among the nondisease chromosomes (Luria and Delbrück 1943; Hästbacka et al. 1992; Hellsten et al. 1993). The Luria-Delbrück formula was used to estimate the genetic distance between the markers giving significant P_{excess} values and the hypothetical LCCS gene. Multipoint analysis adapting linkage disequilibrium was performed with the DISMULT program (Terwilliger 1995). In this method the distances between the analyzed markers are fixed, and the program maximizes the likelihood at a given map position, as a function of the proportion of disease alleles (α values) and the number of generations (n values) since the disease allele has been introduced into the population.

Visual Mapping by FISH

The P1-derived artificial clones (PACs) were isolated from a genomic PAC library kindly provided by P. J. de Jong (Ioannou et al. 1994). The bacterial artificial clones (BACs) were obtained from Genome Systems. The probes were labeled by nick translation with either biotin-11-dUTP (Sigma) or digoxigenin-11-dUTP (Boehringer Mannheim). The size range of the labeled probe fragments was 300–800 bp, as estimated by agarose-gel electrophoresis.

For visual mapping, the metaphase spreads from human peripheral blood lymphocyte cultures were prepared according to standard protocols. Preparation of extended DNA fibers for use as templates has been described in detail elsewhere (Heiskanen et al. 1994, 1996). Fifty to 150 ng of each of the labeled probes was applied, per slide, in the presence of a 10–30-fold excess of unlabeled Cot-1 DNA (Life Technologies). The specific hybridization signals were detected as has been described elsewhere (Heiskanen et al. 1994). Chromosomal DNA was counterstained with 0.025 mg of DAPI (4′-6′diamino-2-phenylindole)/ml, and DNA fibers were counterstained with 5 μg of DAPI/ml (Sigma Chemical). The slides were mounted with antifade solution (Vector Laboratories). Hybridizations were evaluated as described elsewhere Heiskanen et al. 1996).

DNA Sequencing

According to our FISH results, the NGAL gene resides in the vicinity of the marker D9S61, which gave the most significant linkage-disequilibrium values. The PCR products obtained by amplification of the TATA signal region and of seven exons of the NGAL gene were sequenced by means of Sanger's dideoxy-chain termination reaction (Sanger et al. 1977), as described elsewhere (Syvänen et al. 1989) . The TATA signal region and the exons were amplified from two patient samples and one control sample by PCR with intronic primers (European Molecular Biology Loboratory [accession number X99133]), in which the reverse primers were bionytylated. The PCR forward primers were used in the sequencing reaction. The radiolabeled sequence reaction products were separated by denaturing polyacrylamide gels, and the fragments were analyzed by autoradiography.

Results

Genomewide Scan

The initial genome scan was performed with the DNAs of five affected individuals from two families with no known common ancestor throughout six generations, as verified by church records (the five affected individuals are denoted by asterisks in fig. 1). The existence of these two or three affected siblings per family provided us with an opportunity to reconstruct, with a relatively high certainty, the parental haplotypes. Genotyping of 650 polymorphic markers with an average density of 5 cM on autosomes did not reveal, in any of the five affected individuals, a common haplotype on any chromosomal segment. However, the haplotypes of the two affected siblings in family 2 were identical by descent (IBD) for a total of 18 chromosomal regions, and the three siblings in family 3 were IBD for 8 regions. Four of the identified IBD regions were harbored in the same chromosomal regions, although the affected individuals did not share identical alleles. The regions extended 12 cM on chromosome 8, 28 cM on chromosome 9, 23 cM on chromosome 10, and 5 cM on chromosome 18. Linkage analysis using dense marker sets on these four regions in the complete family material of 10 families with 20

affected individuals revealed evidence for linkage between the LCCS and the chromosome 9 markers and excluded the other chromosomal regions.

The results of pairwise linkage analyses obtained with 15 markers on chromosome 9 are shown in table 1. The maximum pairwise LOD score of 4.7 (recombination frequency [θ] .00) was obtained with the marker D9S61. The multipoint linkage analysis revealed the maximum LOD score of 6.5, which peaked between markers D9S1825 and D9S1830 (fig. 2). No evidence of locus heterogeneity was observed by HOMOG program.

The obligatory recombinations restricted the LCCS locus to a 4-cM interval on 9q34. In families 3 and 10, the recombinations in the affected individuals restricted the region to a location telomeric to the marker D9S1825, and one recombination in family 2 in a carrier sibling positioned the LCCS locus within a region centromeric to marker D9S1830. With our small family material, we could not further define the interval for the LCCS locus.

The mother of family 3 was homozygous for the analyzed markers within the region D9S1825–D9S903. To exclude the possibility of loss of heterozygosity in this region, we analyzed the metaphase-chromosome preparations for this mother. The lymphocyte metaphase spreads were hybridized with the BAC and PAC clones, with markers D9S61 and D9S904. Respectively, these probes gave distinct signals on both chromosomes, indicating the presence of this DNA region in both copies of the mother's genome.

Table 1

Pairwise LOD Scores between the LCCS Locus and Markers on 9q, for 10 LCCS Families

	LOD Score at θ =[a]					
Locus	.0	.01	.05	.1	.3	.4
GSN	2.30	2.90	2.20	1.50	.80	.23
D9S1850	−∞	−2.30	−.92	−.39	.09	.03
D9S1829	1.20	1.30	1.43	1.40	1.10	.61
D9S1881	1.80	1.81	1.64	1.19	.66	.19
D9S1825	−∞	.64	1.64	1.75	.36	.10
D9S118	1.70	1.70	1.50	1.20	.40	.10
D9S904	1.70	1.70	1.60	1.40	.50	.20
D9S903	1.30	1.30	1.20	1.00	.40	.10
D9S61	4.70	4.60	4.20	3.60	1.40	.43
D9S752	4.60	4.50	4.00	3.40	1.30	.40
D9S1795	2.20	2.20	2.10	1.80	.70	.20
D9S1831	2.70	2.70	2.40	2.00	.73	.21
D9S1863	3.10	3.00	2.80	2.40	.90	.25
ABL	2.00	2.00	1.90	1.70	.70	.21
D9S179	4.10	4.00	3.60	3.20	1.30	.40
D9S64	3.80	3.70	3.40	3.00	1.20	.40
D9S1830	−∞	3.40	3.60	3.20	1.30	.40

[a] The maximum LOD score for each locus is underlined.

Restriction of the LCCS Region by Ancient-Haplotype Analysis

To restrict the critical LCCS region further, extended haplotypes were built on the basis of alleles detected by polymorphic markers on 9q34. The 3-cM core haplotype 4-4-7-2-1-1-1 (cen-D9S1881-D9S1825-D9S118-D9S904-D9S903-D9S61-D9S752-tel) was observed in 3 (15%) of 20 disease chromosomes. Furthermore, 19 (95%) of the 20 disease chromosomes carried the same restricted core haplotype 1-1 with markers D9S61 and D9S752 separated by 0.5 cM in the genetic maps. The 1-1 haplotype was not observed in any of the 20 nondisease chromosomes. The ancient recombinations restricting the core haplotype thus would define the critical LCCS region as spanning ~0.5 cM between markers D9S903 and D9S61. The haplotypes of disease chromosomes in individual families are given in table 2.

Fine Mapping of the LCCS Region

With the information obtained with the dense marker map on 9q34, we used linkage-disequilibrium analysis to localize the LCCS gene more precisely. The *P* values resulting from the TDT test and the λ values from the likelihood-ratio (LRT) tests are shown in table 2. The most significant *P* values (<.0002) were observed with markers D9S61, D9S752, ABL, and D9S179. To perform the multiple-loci-association analysis, the DISMULT test was used with fixed values of θ (the genetic distance between the markers). The maximum LOD score of 6.7 was observed close to marker D9S61, with an α value of .99 and an n value of 157. These results are suggestive of a single major and old mutation causative for LCCS. When this information was adapted to the Luria-Delbrück formula for markers D9S61 and D9S752, under the assumption of >100 generations as the age of the disease mutation, the critical LCCS region was estimated to be <100 kb from the marker D9S61 (fig. 3).

Physical Map of the LCCS Locus

PAC and BAC clones were isolated from the corresponding libraries by PCR screening with markers D9S904, D9S61, D9S752, D9S1831, and D9S1863. These clones and the cosmid clone for the ABL gene were used as probes in the FISH analysis. Both the metaphase-chromosomal preparations and the extended DNA fibers were used as hybridization targets to determine the order of the clones, as well as to evaluate the coverage of the physical contig in the critical region. The order of the markers was established to be cen-D9S904-D9S61-D9S752-D9S1831-D9S1863-ABL-tel. The clones for markers D9S61 and D9S752 were assigned very close to each other, whereas the distance between the clones for D9S752

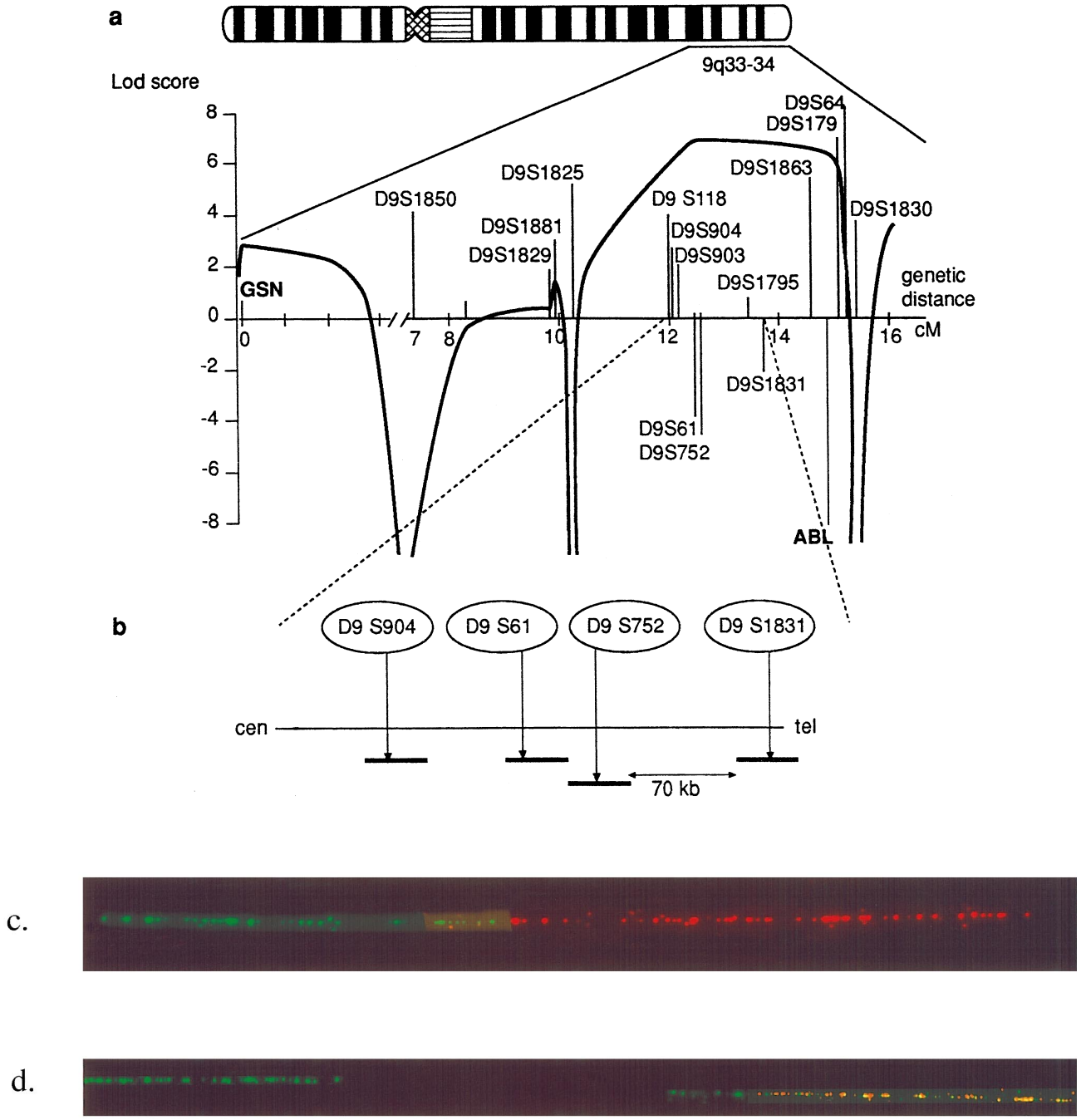

Figure 2 *a*, Results of multipoint linkage analysis between LCCS and markers on chromosome 9q33-34, positioning the LCCS locus between markers D9S1825 and D9S1830. The markers and the genetic distances between them are as follows: GSN–7 cM–D9S1850–2.5 cM–D9S1829–0.2 cM–D9S1881–0.1 cM –D9S1825–2 cM–D9S118 –0.5 cM–D9S904–0.1 cM–D9S903–0.1 cM–D9S61–0.1 cM–D9S752 –0.9 cM–D9S1795–0.3 cM–D9S1831–0.9 cM–D9S1863–0.3 cM–ABL–0.1 cM–D9S179–0.1 cM–D9S64–0.1 cM–D9S1830). *b*, Schematic illustration of the preliminary physical map is shown over the critical LCCS region. The PAC and BAC clones are shown under the horizontal axis. The ovals represent polymorphic microsatellites used to isolate the clones. The sizes of the clones and the distances between them are not according to scale. *c*, Fiber FISH–based fine-resolution visual mapping of BAC clones for D9S61 (*green*) and D9S752 (*red*). *d*, Fiber FISH–based fine-resolution visual mapping of BAC clones for D9S752 (*green*) and of the PAC clone for D9S1831 (*yellow*). In these analyses, the BAC clones for D9S61 and D9S752 proved to overlap each other. The physical distance between the BAC clone for D9S752 and the PAC clone for D9S1831 is estimated to be 70 kb.

Table 2

Extended Haplotypes for 11 Markers in the LCCS Locus

Family	D9S1825 HRR λ = .58 TDT P = .0013	D9S118 HRR λ = .38 TDT P = .0018	D9S904 HRR λ = 0 TDT P = .05	D9S903 HRR λ = 0 TDT P = .03	D9S61 HRR λ = .91 TDT $P = 2.0 \times 10^{-7}$	D9S752 HRR λ = .9 TDT $P = 1.5 \times 10^{-6}$	D9S1795 HRR λ = 0 TDT P = .1	D91831 HRR λ = 0 TDT P = .004	D9S1863 HRR λ = 0 TDT P = .02	ABL HRR λ = .58 TDT P = .0002
1	4	7	2	1	1	1	2	3	2	2
	4	2	2	1	1	1	1	3	1	2
2	4	2	2	1	1	1	3	4	1	2
	4	7	2	1	1	1	1	2	2	2
3	3	7	2	1	1	1	2	3	2	2
	4	7	2	1	1	1	1	2	2	2
4	4	4	2	1	1	1	3	2	5	2
	4	7	2	1	3	4	2	4	1	3
5	4	7	2	1	1	1	3	ND	2	1
	4	7	2	1	1	1				
6	3	7	2	1	1	1	2	ND	2	2
	4	3	2	1	1	1	3	1	2	1
7	3	6	1	1	1	1	2	ND	2	2
	4	7	1	2	1	1	3	ND	5	2
8	4	7	2	1	1	1	3	3	1	1
	2	2	2	1	1	1	ND	4	1	4
9	4	7	2	1	1	1	1	ND	4	2
	5	1	2	1	1	1	4	ND	2	2
10	ND	7	2	1	1	1	2	ND	ND	ND
	ND	7	2	1	1	1	1	ND	ND	ND

NOTE.—ND = not determined.

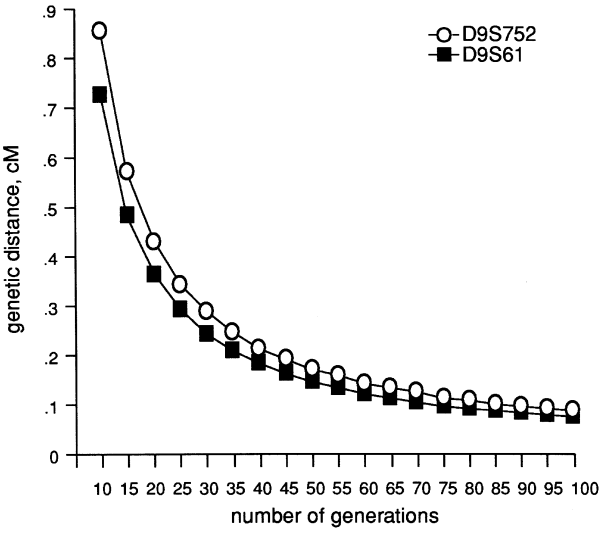

Figure 3 Results obtained with the Luria-Delbrück formula, for markers D9S752 and D9S61. On the basis of this formula, the approximation of the distance between the LCCS locus and markers D9S61 and D9S752 is given as a function of the number of the generations.

and D9S1831 was approximated to be 70 kb on extended DNA fibers (fig. 2*c* and *d*).

Analysis of Candidate Genes on 9q34

The FISH analysis of metaphase chromosomes (fig. 4) with the PAC clone containing the NOTCH1 gene and the cosmid for the ABL gene assigned the NOTCH1 gene to a region telomeric to the ABL gene, positionally excluding it from the critical LCCS region and ruling it out as a causative gene for LCCS. The FISH analysis of the physical PAC clone containing the second candidate gene, NGAL, demonstrated proximity of this gene to marker D9S61, making the NGAL gene a positional candidate for LCCS. The PCR products of all seven exons and of 150 bp of the promoter region, including the TATA-signal region of NGAL, were analyzed by sequencing of the genomic DNA, and no variations between the two affected individuals and one control sample were detected in the sequence analysis.

Discussion

We have reported here the assignment of the LCCS locus to a restricted region on chromosome 9q34. The chromosomal region was identified by use of only five DNA samples from patients from two unrelated families in the initial genome scan. This was justified because of the assumption of a single causative mutation underlying LCCS, suggested by the clustering of cases in the more recently settled area of northeastern Finland. We analyzed a total of 650 polymorphic markers, but no single chromosomal segment could be identified that was shared by all five affected individuals. However, we were able to identify four chromosomal regions that were IBD in the siblings, but the alleles differed between the two families; a conventional linkage study in the complete DNA material of 10 families revealed evidence of linkage for chromosome 9q34 and excluded the other three regions. It was surprising that the three siblings of one family shared a total of only eight chromosomal segments. Our previous (Pekkarinen et al. 1998) and present findings suggest that, in the locus search in recessive diseases with complete penetrance, it initially is sufficient to genotype only two or three affected siblings, to identify the chromosomal segments of interest, which then can be further analyzed in the complete DNA material of the family.

Shortcut strategies to assign disease loci have been described elsewhere; they include use of samples from three or four patients who are distant relatives (Nikali et al. 1995), as well as the pooling of DNA samples (Arbour et al. 1997). LCCS families could not be traced back to common ancestors; but they were regionally clustered, which suggests that such an ancestor exists. We would not have been able, with a routinely adapted density of DNA markers, to detect the linkage either by pooling the DNA samples or by analyzing a single patient per family, because of the shortness of the chromosomal region shared by the affected fetuses.

The observed obligatory recombinations in the LCCS families restricted the locus to a 4-cM region. Analysis of the ancient core haplotype restricted this critical chromosomal region further, to an ~0.5-cM region between the markers D9S903 and D9S61, and the detected linkage disequilibrium further restricted it to <100 kb in the vicinity of D9S61. The short genetic interval revealing linkage disequilibrium in LCCS alleles supports the scenario of the early introduction of the LCCS mutation into this population (de la Chapelle 1993; Peltonen et al. 1995). However, the clustering of the disease gene within the recently settled northeastern part of Finland, as well as the clustering of grandparents' birthplaces, suggests the opposite—a late introduction of the gene into the Finnish population (Vuopala and Herva 1994). This discrepancy is peculiar and exceptional, compared with what is observed in other Finnish diseases. In the case of infantile-onset spinocerebellar ataxia, linkage disequilibrium was detected over a 2-cM region, and the genealogical search combined with the haplotype analyses suggested that the mutation was introduced some 40 generations ago and that the mutation then spread with the main migration movement from western to east-

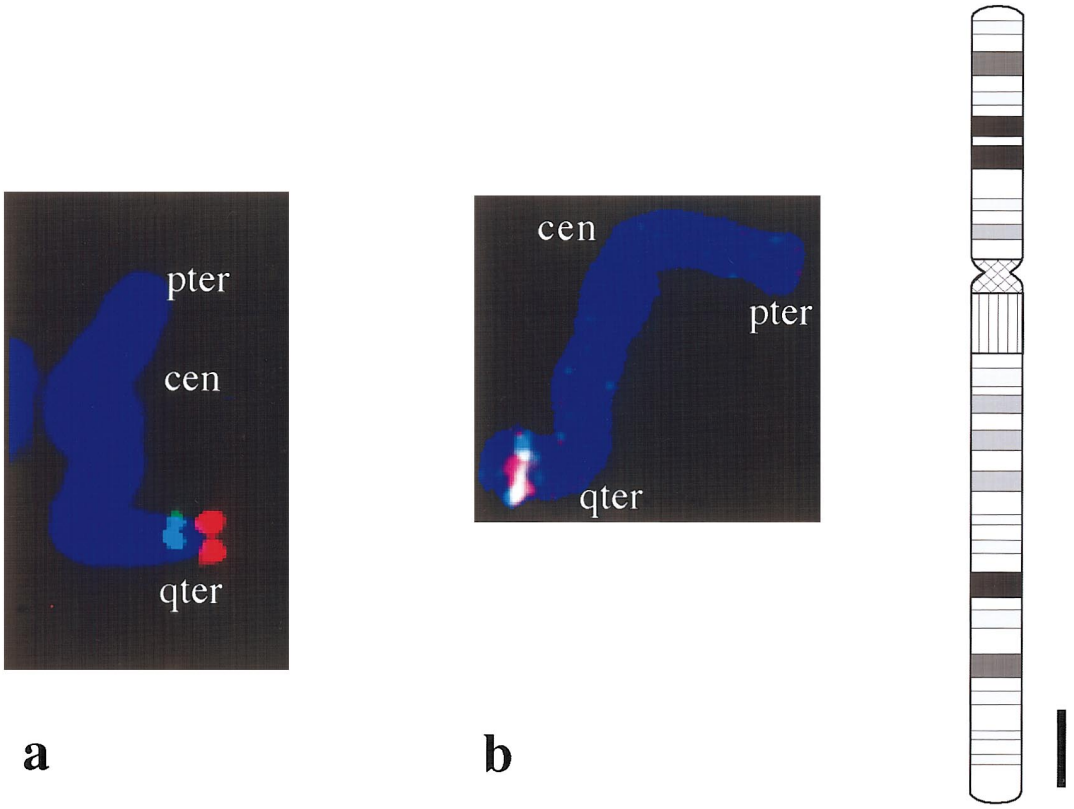

Figure 4 *a,* Results of FISH analysis of metaphase chromosomes, with clones for the NOTCH1 gene (*red*) and the ABL gene (*green*) The NOTCH1 clone assigns a more-telomeric region than does the ABL clone, localizing the NOTCH1 to the telomeric border of the LCCS region, which is restricted by obligatory recombinations. *b,* Results of metaphase FISH analysis, which indicate the vicinity of the clones for the NGAL gene (*red*) and for marker D9S61 (*green*).

ern Finland (Varilo et al. 1996*a*). Another Finnish disease, the variant form of infantile neuronal ceroid lipofuscinosis is still clustered within a small region of southern Ostrobothnia, and linkage disequilibrium has been detected over an 11-cM interval. This is in agreement with the genealogical tracing of ancestors to the same community, suggesting a relatively new mutation introduced some 20-30 generations ago (Varilo et al. 1996*b*). In both cases, the genealogy and linkage-disequilibrium results predict a similar age range for the mutation.

The population history of northern Finland, together with the clustering of LCCS cases, supports the idea of the late introduction of this disease gene. The northern and eastern parts of Finland were inhabited during the 16th and 17th centuries, after the east-to-west migration (Solantie 1988). This movement spread the rare genes to internal isolates, where the disease-gene frequencies remained stable until the present century (Norio et al. 1973). We assume that the ancestors carrying the LCCS mutation arrived in northeastern Finland during the late 17th century, when this region was settled by small immigrants groups from the western part of Finland. However, on the basis of linkage disequilibrium, the predicted age of the ancestor mutation would be >100 generations. The possibility of several founders carrying the same LCCS mutation and inhabiting this part of Finland at the same time period cannot be excluded, nor can carriers who would have arrived from Russia and who might have brought an old mutation into eastern Finland.

The nature of the chromosomal region of LCCS also may explain the discrepancy between the expected mutational age and a short segment of linkage disequilibrium. The LCCS locus shares the chromosomal region of 9q34 with the neoplasia-associated chromosomal translocation locus (Carrol et al. 1987), a region with a high frequency of recombination. Furthermore, the LCCS locus is telomeric, a location prone to recombination. When the physical distances to the genetic interval in this region are compared, the clones for markers D9S752 and D9S1831 are separated by 70 kb, on the

basis of fiber FISH, whereas the genetic distance between them is >1.2 cM, suggesting a high θ value in this DNA region. Therefore the shortness of the core haplotype may reflect the high number of recombinations in this region rather than the number of generations elapsed.

NOTCH 1 is a large transmembrane protein in which a disease-associated mutation, t(7;9) translocation, initially was described in a T-cell leukemia (Ellisen et al. 1991). Studies of the oncogenic activity of the truncated NOTCH 1 have demonstrated that NOTCH 1 plays a role in the determination of cell fate during early fetal development (Lardelli et al. 1995) NOTCH 1 protein is suggested to be essential for signal transduction (Lieber et al. 1993), and NOTCH 1^{D1} knockout mice show high lethality (Conlon et al. 1995). All these findings have made the NOTCH1 a good candidate gene for LCCS. However, our FISH data clearly assigned the NOTCH1 to a region outside the critical chromosomal region, thereby excluding it as a causative gene of LCCS.

The NGAL belongs to the lipocalin superfamily (Bundgaard et al. 1994). It is believed to bind small lipophilic molecules and to act as a modulator of inflammation. It is mitogenic and enhances cell growth and proliferation. Neither the ligand nor the receptor for this extracellular protein has been characterized (Flower 1994). The gene is known to be expressed in fetal spleen and lung, as well as in adult bone marrow and tissues involved in the inflammatory response. (Cowland and Borregaard 1997). The expression pattern of the protein in the fetal CNS is not known. Our sequence analysis of the coding region of the NGAL gene did not reveal differences in LCCS patients compared with controls. However, neither nucleotide changes in other parts of the gene nor the possibility of gene-dosage effect of this interesting gene, known to be involved to cell regulation, can be excluded.

LCCS is a motoneuron disease, as is spinal muscular atrophy (SMA), a disease that occasionally presents with artrogryposis and fetal akinesia sequence. SMA also is known to be associated with anterior-horn-cell loss (Burglen et al. 1996; Devriendt et al. 1996; Rudnik-Schoneborn et al. 1996). In this disorder, however, the descending tracts of the spinal cord are preserved. In an earlier report, we excluded the SMA locus at 5q as being the LCCS locus (Vuopala et al. 1995). LCCS resembles more the adult motoneuron disease amyotrophic lateral sclerosis, in which the motoneurons of the spinal cord often are seen to be affected, whereas in LCCS the degeneration of motoneurons already occurs during fetal development (Herva et al. 1988; Vuopala et al. 1995). Assignment of the LCCS locus provides a tool for isolation of the gene underlying lethal motoneuron disease. Identification of the gene defect is necessary for understanding the pathogenesis of LCCS and the normal development of motoneurons. It will also offer an opportunity for development of a mouse model for motoneuron disease, facilitating detailed monitoring of the disease process at the tissue level.

Acknowledgments

We would like to thank the LCCS families for their willingness to participate in this study. We are grateful to Dr. Petra Pekkarinen for her advice in the statistical analyses and to Dr. Ann-Christine Syvänen for her advice in DNA extraction. This study was supported by the Hjelt Fond of the Pediatric Research Foundation and by the Academy of Finland.

Electronic-Database Information

Accession numbers and URLs for data in this article are as follows:

Online Mendelian Inheritance in Man (OMIM), http://www.ncbi.nlm.nih.gov/omim (for LCCS [MIM 253310])
European Molecular Biology Laboratory, http://www.ebi.ac.uk/htbin/emblfetch?X99133 (for NGAL gene sequence)

References

Arbour NC, Zlotogora J, Knowlton RG, Merin S, Rosenmann A, Kanis AB, Rokhlina T, et al (1997) Homozygosity mapping of achromatopsia to chromosome 2 using DNA pooling. Hum Mol Genet 6:689–694

Bundgaard JR, Sengelov H, Borregaard N, Kjeldsen L (1994) Molecular cloning and expression of a cDNA encoding NGAL: a lipocalin expressed in human neutrophils. Biochem Biophys Res Commun 202:1468–1475

Burglen L, Amiel J, Viollet L, Lefebvre S, Burlet P, Clermont O, Raclin V, et al (1996) Survival motor neuron gene deletion in the arthrogryposis multiplex congenita-spinal muscular atrophy association. J Clin Invest 98:1130–1132

Carroll AJ, Raimondi SC, Williams DL, Behm FG, Borowitz M, Castleberry RP, Harris MB, et al (1987) Nonrandom chromosome abnormality in childhood B-cell precursor acute lymphoblastic leukemia: a pediatric Oncology Group Study. Blood 70:1962–1965

Chan P, Simon-Chazottes D, Mattel MG, Guenet JL, Salier JP (1994) Comparative mapping Of lipacalin genes in human and mouse: four genes for complement C8 gamma chain, prostaglandin-D-synthase, oncogene-24P3 and prostagem-associated endometrial protein map to HSA9 and MMU2. Genomics 23:145–150

Conlon RA, Reaume AG, Rossant J (1995) Notch 1 is required for the coordinate segmentation of somites. Development 121:1533–1545

Cowland JB, Borregaard N (1997) Molecular characterization and pattern of tissue expression of the gene for neutrophil gelatinase-associated lipocalin from humans. Genomics 45: 17–23

de la Chapelle A (1993) Disease mapping in isolated human populations: the example of Finland. J Med Genet 30: 857–865

Devriendt K, Lammens M, Schollen E, Van Hole C, Dom R, Devlieger H, Cassiman JJ, et al (1996) Clinical and molecular genetic features of congenital spinal muscular atrophy. Ann Neurol 40:731–738

Ellisen LW, Bird J, West DC, Soreng AL, Reynolds TC, Smith SD, Sklar J (1991) TAN-1, the human homolog of the Drosophila notch gene, is broken by chromosomal translocations in T lymphoblastic neoplasms. Cell 66:649–661

Flower D (1994) The lipocalin protein family: a role in cell regulation. FEBS Lett 354:7–11

Hästbacka J, de la Chapelle A, Kaitila I, Sistonen P, Weaver A, Lander E (1992) Linkage disequilibrium mapping in isolated founder populations: diastrophic dysplasia in Finland. Nat Genet 2:204–211 (erratum, Nat Genet 2:343 [1992])

Heiskanen M, Kallioniemi O, Palotie A (1996) Fiber-FISH: experiences and a refined protocol. Genet Anal 12(5–6): 179–184

Heiskanen M, Karhu R, Hellsten E, Peltonen L, Kallioniemi OP, Palotie A (1994) High resolution mapping using fluorescence in situ hybridization (FISH) to extended DNA fibers prepared from agarose-embedded cells. Biotechniques 17: 928–934

Hellsten E, Vesa J, Speer MC, Makela TP, Jarvela I, Alitalo K, Ott J, et al (1993) Refined assignment of the infantile neuronal ceroid lipofuscinosis (INCL, CLN1) locus at 1p32: incorporation of linkage disequilibrium in multipoint analysis. Genomics 16:720–725

Herva R, Conradi NG, Kalimo H, Leisti J, Sourander P (1988) A syndrome of multiple congenital contractures: neuropathological analysis on five fetal cases. Am J Med Genet 29:67–76

Herva R, Leisti J, Kirkinen P, Seppanen U (1985) A lethal autosomal recessive syndrome of multiple congenital contractures. Am J Med Genet 20:431–439

Houwen RH, Baharloo S, Blankenship K, Raeymaekers P, Juyn J, Sandkuijl LA, Freimer NB (1994) Genome screening by searching for shared segments: mapping a gene for benign recurrent intrahepatic cholestasis. Nat Genet 8:380–386

Iannou PA, Amemiya CT, Garnes J, Kroisel PM, Shizuya H, Chen C, Batzer MA, et al (1994) A new bacteriophage P1-derived vector for the propagation of large human DNA fragments. Nat Genet 6:84–89

Isola J, De Vries S, Chu L, Ghazvini S, Waldman F (1994) Analysis of changes in DNA sequence copy number by comparative genomic hybridization in archival paraffin-embedded tumor samples. Am J Pathol 145:1301–1308

Lardelli M, Williams R, Lendahl U (1995) Notch-related genes in animal development. Int J Dev Biol 39:769–780

Larsson C, Lardelli M, White I, Lendahl U (1994) The human NOTCH1, 2, and 3 genes are located at chromosome positions 9q34, 1p13-p11, and 19p13.2-p13.1 in regions of neoplasia-associated translocation. Genomics 24:253–258

Lathrop GM, Lalouel JM (1984) Easy calculations of lod scores and genetic risks on small computers. Am J Hum Genet 36:460–465

Lathrop GM, Lalouel JM, Julier C, Ott J (1984) Strategies for multilocus linkage analysis in humans. Proc Natl Acad Sci USA 81:3443–3446

Lathrop GM, Lalouel JM, White RL (1986) Construction of human linkage maps: likelihood calculations for multilocus linkage analysis. Genet Epidemiol 3:39–52

Lieber T, Kidd S, Alcamo V, Corbin M, Young MW (1993) Antineurogenic phenotypes induced by truncated Notch proteins indicate a role of signal transduction and may point to novel a function for Notch in nuclei. Genes Dev 7: 1949–1965

Luria SE, Delbrück M (1943) Mutations of bacteria from virus sensitivity to virus resistance. Genetics 28:491–511

Nikali K, Suomalainen A, Terwilliger J, Koskinen T, Weissenbach J, Peltonen L (1995) Random search for shared chromosomal regions in four affected individuals: the assignment of a new hereditary ataxia locus. Am J Hum Genet 56: 1088–1095

Norio R, Nevanlinna HR, Perheentupa J (1973) Hereditary diseases in Finland; rare flora in rare soil. Ann Clin Res 5: 109–141

Ott J (1986) linkage probability and its approximate confidence interval under possible heterogeneity. Genet Epidemiol Suppl 1:251–257

Ott J (1989) Computer-simulation methods in human linkage analysis. Proc Natl Acad Sci USA 86:4175–4178

Pekkarinen P, Hovatta I, Hakola P, Järvi O, Kestilä M, Lenkkeri U, Adolfsson R, et al (1998) Assignment of the locus for PLO-SL, a frontal-lobe dementia with bone cysts, to 19q13. Am J Hum Genet 62:362–372

Peltonen L, Pekkarinen P, Aaltonen J (1995) Messages from isolate: lessons from Finnish gene pool. Biol Chem Hoppe-Seyler 376:697–704

Rudnik-Schoneborn S, Forkert R, Hahnen E, Wirth B, Zerres K (1996) Clinical spectrum and diagnostic criteria of infantile spinal muscular atrophy: further delineation on the basis of SMN gene deletion findings. Neuropediatrics 27:8–15

Sanger F, Nicklen S, Coulson AR (1977) DNA sequencing with chain-terminating inhibitors. Proc Natl Acad Sci USA 74: 5463–5467

Sheffield V, Weber J, Buetow K, Murray J, Viles K, Gastier J (1995) A collection of tri- and tetranucleotide repeat markers used to generate high quality, high resolution human genome-wide linkage maps. Hum Mol Genet 4:1837–1844

Solantie R (1988) Climatic conditions for the cultivation of rye with reference to the history of settlement in Finland. Fennoscandia Archaelogia 5:3–20

Syvänen A-C, Sajantila A, Aalto-Setälä K, Kontula K, Söderlung H (1989) Direct sequencing of affinity-captured amplified human DNA: application to the detection of apolipoprotein E polymorphism. FEBS Lett 258:71–72

Terwilliger JD (1995) A powerful likelihood method for the analysis of linkage disequilibrium between trait loci and one or more polymorphic marker loci. Am J Hum Genet 56: 777–787

Varilo T, Nikali K, Suomalainen A, Lonnqvist T, Peltonen L (1996*a*) Tracing an ancestral mutation: genealogical and haplotype analysis of the infantile onset spinocerebellar ataxia locus. Genome Res 6:870–875

Varilo T, Savukoski M, Norio R, Santavuori P, Peltonen L, Järvelä I (1996*b*) The age of human mutation: genealogical and linkage disequilibrium analysis of the CLN5 mutation in the Finnish population. Am J Hum Genet 58:506–512

Vuopala K, Herva R (1994) Lethal congenital contracture syn-

drome: further delineation and genetic aspects. J Med Genet 31:521–527

Vuopala K, Leisti J, Herva R (1994) Lethal arthrogryposis in Finland—a clinicopathological study of 83 cases during thirteen years. Neuropediatrics 25:308–315

Vuopala K, Makela-Bengs P, Suomalainen A, Herva R, Leisti J, Peltonen L (1995) Lethal congenital contracture syndrome (LCCS), a fetal anterior horn cell disease, is not linked to the SMA 5q locus. J Med Genet 32:36–38

Weeks DE, Ott J, Lathrop GM (1990) SLINK: a general simulation program for linkage analysis. Am J Hum Genet Suppl 47:A204